Full-bandwidth adaptive waveform inversion at the reservoir

Henry A. Debens & Fabio Mancini, Woodside Energy Ltd; Mike Warner & Lluís Guasch, S-CUBE London*

Summary

Adaptive waveform inversion (AWI) is one of a new breed of full-waveform inversion (FWI) algorithms that seek to mitigate the effects of cycle skipping (Warner & Guasch, 2016). The phenomenon of cycle skipping is inherent to the classical formulation of FWI, owing to the manner in which it tries to minimize the difference between oscillatory signals. AWI avoids this by instead seeking to drive the ratio of the Fourier transform of the same signals to unity. One of the strategies most widely employed by FWI practitioners when trying to overcome cycle skipping, is to introduce progressively the more nonlinear components of the data, referred to as multiscale inversion. Since AWI is insensitive to cycle skipping, we assess here whether this multiscale approach still provides an appropriate strategy for AWI.

Introduction

Full-waveform inversion is now considered by many to be a routine tool for exploration and development (e.g. Mancini et al., 2015). This is because of FWI's ability to generate high-resolution high-fidelity models of subsurface properties, principally acoustic velocity, notwithstanding the large computational costs associated where runtimes increase as the fourth power of the maximum frequency.

FWI is not however without its limitations. Classical FWI seeks to minimize, in a least-squares sense, the difference between observed and modeled seismic data (Tarantola, 1984). Because seismic data are band-limited and oscillatory, the sum of the squares of their differences will pass through a local minimum whenever one dataset is shifted in time by an integer number of cycles with respect to the other. The resultant phenomenon of cycle skipping is one of the principal roadblocks to FWI's widespread application to seismic data.

AWI reformulates the inversion problem so that it seeks not to drive the difference of the two datasets to zero but instead seeks to drive their ratio to unity. In practice, this ratio is formulated in the frequency domain where AWI then becomes equivalent to designing a wiener filter that matches one dataset to the other, and the inversion seeks to drive this filter towards a unit-amplitude, zero-lag, band-limited, delta function. This formulation does not pass through a local minimum when the two datasets differ by an integer number of wave cycles, and so it is entirely unaffected by cycle skipping.

Although it is able to circumvent cycle skipping, AWI possesses no special immunity to other causes of local minima in FWI, for example the misidentification of multiples as primaries or the misidentification of one branch of a multi-pathed arrival with another. Some of these non-cycle-skipped causes of local minima become more likely at higher frequencies.

Given these characteristics, it is not immediately clear that the multiscale approach commonly applied in conventional FWI (Bunks et al., 1995) will still provide the most effective strategy for AWI. Its use in FWI is essential to avoid cycle skipping unless the starting model is extremely accurate, but in AWI cycle skipping is no longer a consideration. This raises the question as to whether traditional approaches that move from low to high frequency during FWI are still appropriate for AWI. If it is the case that the multiscale approach is no longer required, then this reduces the requirement to capture ultra-low frequency data for waveform inversion, and can avoid the cost of ensuring that this portion of the data is clean.

Field data example

To explore the behavior of AWI with respect to inversion bandwidth, we designed a series of experiments using a subset of narrow azimuth towed-streamer data collected over the Rakhine Basin, offshore Myanmar. This dataset, acquired in 2014, used flip-flop air gun arrays, deployed 50 m apart, fired sequentially every 50 m, into ten 7-km cables towed at 15 m depth. The resultant data were high density and of high quality, with good low-frequency content down to the hydrophone low-cut filter at 3 Hz. The target was an accumulation of biogenic gas within a tertiary clastic reservoir thought to have been deposited by the Ganges-Brahmaputra system (Harrowfield, 2015).

The data were minimally preprocessed for waveform inversion. Swell noise was removed, and incoherent and linear noise were filtered from the low-frequency component. The data were then low-pass filtered and decimated in the receiver domain, before being muted ahead of the first arrivals. For FWI, reflection events arriving after 6 s were muted; for AWI no such bottom mute was applied. From one of these preprocessed sail lines, which passed directly over the target and near to a recent exploration wellbore, a single 2D gun-cable combination was extracted. The cable was feathered by up to 8°.

A source wavelet was derived from numerical modeling of the air gun array, corrected in phase and amplitude for 2D propagation. The initial velocity model was based on an early iteration of reflection traveltime tomography, scaled to checkshot data from the nearby well. The position and

reflectivity of the water bottom was refined by modeling synthetic gathers at regular intervals. A VTI anisotropy model was derived using residual moveout on Kirchhoff offset-domain common-image gathers (ODCIGs) migrated using the initial model, and the depth to a marker horizon in these ODCIGs relative to the nearby well.

Results

The first experiment was to compare the results of AWI, undertaken without using multiscale inversion, when using different bandwidths of input data. This was done to assess the frequency at which full-bandwidth AWI breaks down, and to determine whether different bandwidths produce comparable results. Figure 1 shows the results of four AWI runs using input data that had been low-pass filtered at 5, 11, 23 and 47 Hz, respectively. Each inversion used a starting model similar to that shown in Figure 2a, identical parameterization and 80 iterations using the full bandwidth of the input data.

As would be expected, the main difference between each run is the resolution captured by the inversion. Figures 1a-c show broadly the same features: a low-velocity, horizontal, laterally-extensive reservoir at approximately 3 km depth, a number of shallow gas pockets in an otherwise benign overburden, and simple horizontal stratigraphy. The final inversion, Figure 1d, however does not capture the reservoir and is dominated by high-frequency dipping artefacts in the shallow section. Similar noise is also present at a lower spatial frequency in Figure 1c below 3 km, but is less prevalent; the same noise does not obviously exist in Figures 1a or 1b.

In a second experiment, Figure 2, we compared full-bandwidth AWI and FWI at 23 Hz with the results of conventional multiscale FWI, beginning at 3 Hz and running up to 23 Hz. For this test, shallow velocities in the starting model, Figure 2a, were reduced by 1.5%. This is sufficient to introduce cycle skipping into the data for full-bandwidth FWI. For AWI, in order to avoid the generation of sub-vertical noise at depth, we smoothed the model partway through the inversion before continuing. This smoothing increased with depth, and was predominantly horizontal.

The results of the smoothed full-bandwidth AWI are shown in Figure 2b; comparison with Figure 1c shows the effect of the smoothing in suppressing the noise. Figure 2c shows the results of applying full-bandwidth FWI at 23 Hz. This model is now severely compromised by cycle skipping and there is significant spurious structure around and above the reservoir, even in the shallow subsurface. This is unsurprising; the starting model is not especially accurate and conventional FWI is not designed to begin at these high frequencies from an imperfect starting model.

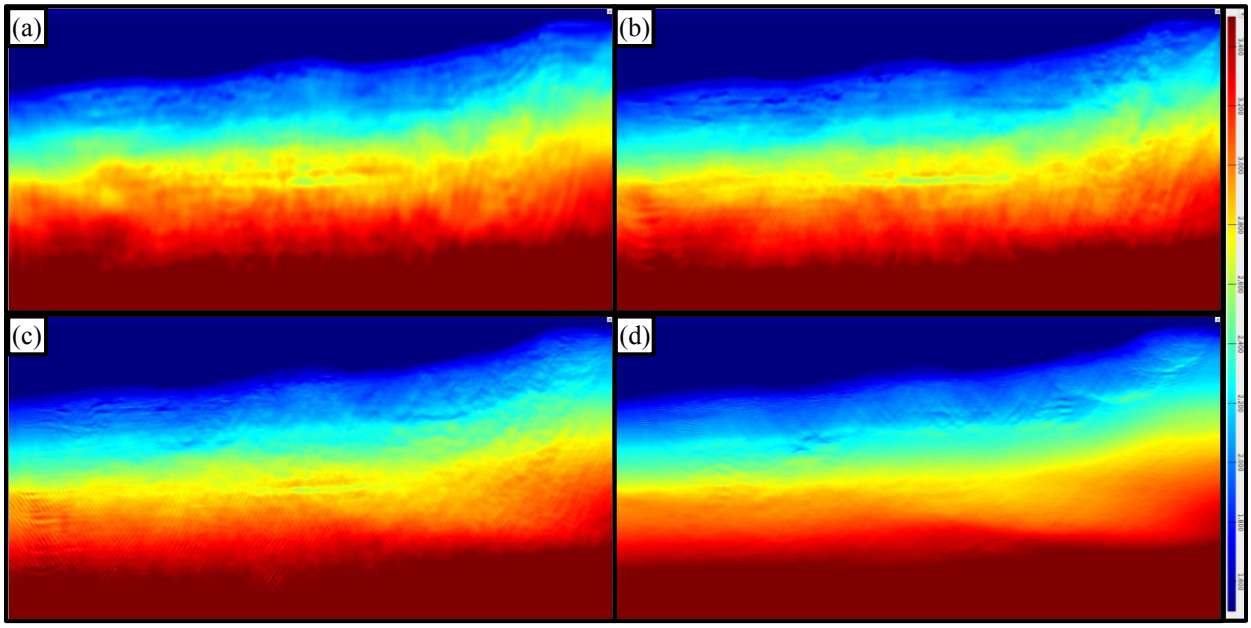

Figure 1: Full-bandwidth AWI results, using low-pass filters with corner frequencies of: (a) 5 Hz, (b) 11 Hz, (c) 23 Hz, and (d) 47 Hz. Each inversion used a spatial filter of identical scale length applied to the AWI gradient.

Using multiscale FWI, Figure 2d, largely avoids the effects of cycle skipping, and produces a more geologically realistic model, particularly in the first 1.5 km below mudline. The reservoir in Figure 2d appears fragmented at its fringes, with suggestions of gas migration into the overburden. Full-bandwidth AWI converges to a similar solution in the shallow section, but it produces a flatter reservoir that agrees closely with the reflection image.

Full-bandwidth AWI and multiscale FWI also differ in the impact of the limited data fold towards the margins of the model. Spurious updates in this region are stronger in the FWI results than in AWI, most likely because of the narrower aperture of the AWI impulse response. In the left-hand side of Figure 2d, in particular, these sweeping artefacts appear to merge into geology, placing uncertainty on the model update here, and impacting migration quality.

Another noticeable difference between the two results is the shape and position of the target reservoir. The reservoir appears more central and flatter in the AWI result than the multiscale FWI. One concern with the AWI model is the presence of broad bowl-like features in the shallow subsurface, similar in appearance to migration aperture artefacts in imaging. Comparable structures are prominent in Figure 1d, where AWI has clearly gone awry, suggesting that these are likely to be spurious.

In an effort to assess which of Figures 2b and 2d is a more accurate representation of the true subsurface, the data were demultipled, deghosted and zero-phased, and migrated using Kirchhoff prestack depth migration (PreSDM). The resultant full stack sections are displayed in Figure 3, overlain on the respective velocity models used to migrate the data. Whilst the differences between the images themselves are subtle, the AWI result, Figure 3b, appears to correlate significantly better with its stack. As the image and model were generated using two quite distinct regimes of wavefield propagation, this agreement suggests that the AWI model provides a reliable account of the geology. The AWI migration result is also generally flatter and more regular.

ODCIGs were generated as a byproduct of the PreSDM, Figure 4. It can be seen that the multiscale FWI gathers contain non-systematic errors throughout. It is especially noticeable that the gathers in the weaker lower-half of the FWI section are under migrated, suggesting that the FWI model has not been able to recover from the perturbation that was introduced deliberately into the starting model. The AWI gathers are flatter, brighter, and more continuous in form. This suggests that the AWI model is indeed more kinematically accurate than its multiscale FWI counterpart.

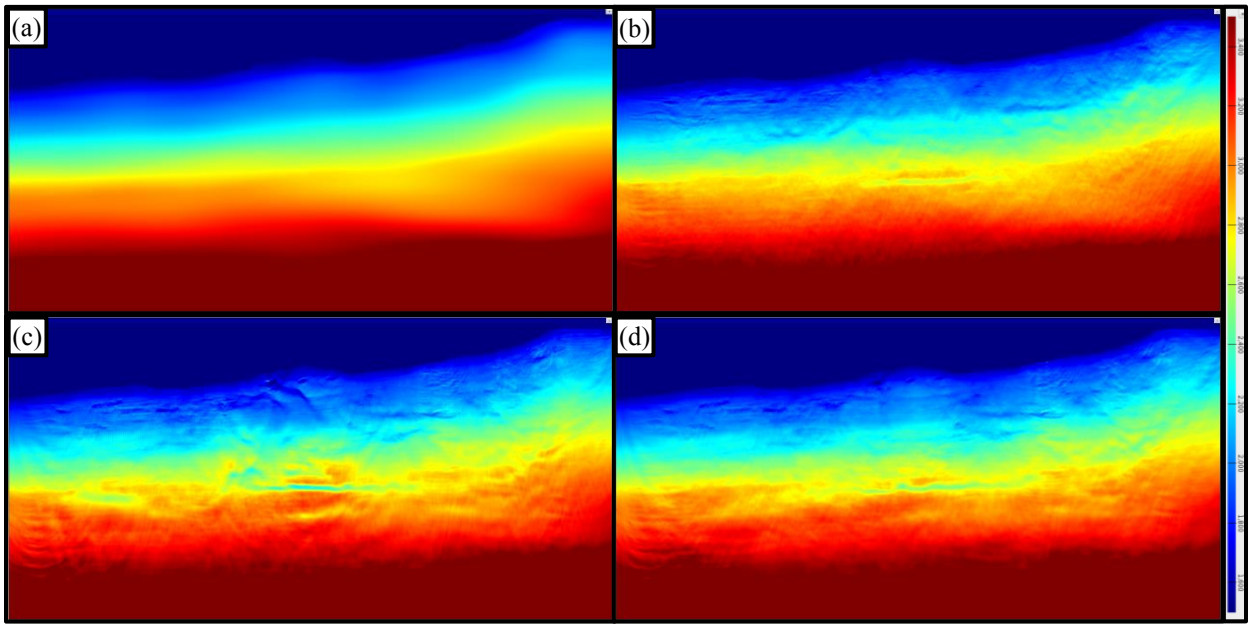

Figure 2: (a) Early-stage reflection tomography model, adjusted by 1.5%, used as a starting model; (b) full-bandwidth AWI model at 23 Hz; (c) full-bandwidth FWI model at 23 Hz; and (d) multiscale FWI model increasing by stages from 3 to 23 Hz.

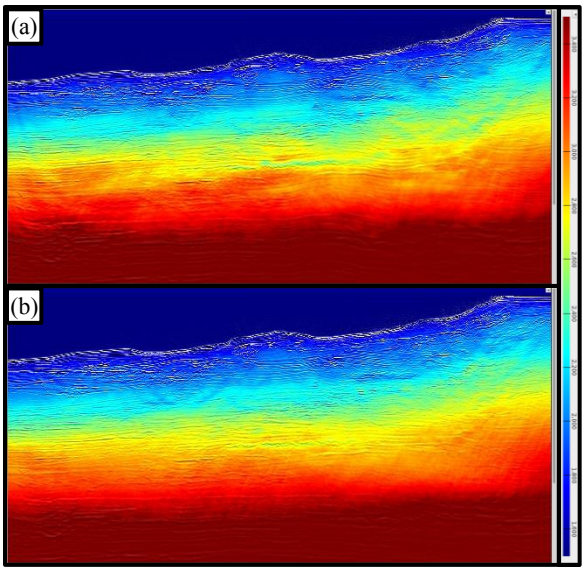

Figure 3: (a) Multiscale FWI and (b) full-bandwidth AWI inversion results after 95 total iterations with PreSDM overlay. Both sections are 27.5 km in length.

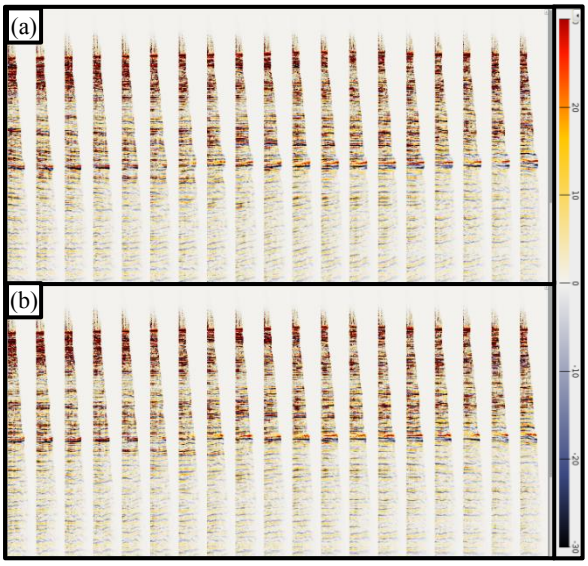

Figure 4: Kirchhoff PreSDM ODCIGs generated using: (a) multiscale FWI (Figure 2d) and (b) full-bandwidth AWI (Figure 2b). Each ODCIG is 150 m apart and has had an outer angle mute applied at 50°.

Discussion and conclusions

AWI is a powerful new approach to waveform inversion that circumvents the phenomena of cycle skipping. The manner in which AWI and similar domain-extension techniques appear set to advance waveform inversion capabilities requires a corresponding reassessment of the optimal strategy for successful and commercially efficient waveform inversion. One such strategy is Bunks et al.'s (1995) multiscale approach designed to accentuate the more linear low-frequency component of the wavefield, and as the inversion converges, gradually introduce the more nonlinear high-frequency component.

AWI does not require this approach in order to mitigate cycle skipping. When using only a moderately accurate starting model, full-bandwidth AWI at 23 Hz appears able to generate a velocity model that produces superior migration outcomes when compared to conventional multiscale FWI iterated from 3 to 23 Hz. Full-bandwidth FWI at 23 Hz of the same data of course fails entirely. Despite its insensitivity to cycle skipping, AWI is not able to begin inversion at frequencies as high as 47 Hz, at least for this quality of starting model. Given a better starting model though, AWI should be able to achieve even this.

A major benefit of AWI is a reduced reliance on low-frequency data to begin waveform inversion. These data are expensive to acquire and require additional processing effort to ensure that their signal-to-noise is suitable for waveform inversion. Although we have shown that full-bandwidth AWI can be effective, we do not advocate that AWI should normally begin at frequencies as high as 23 Hz. Typically we obtain the best outcome from AWI by starting at some intermediate frequency, lower than 23 Hz, but well above the 3 Hz that has become typical for FWI.

AWI has the potential to be integrated with and lend its benefits to other waveform inversion frameworks. An example of such is the combined local and global inversion for anisotropy parameters (Debens et al., 2015), where the use of AWI provides resilience against the effects of local minima related to cycle skipping.

Acknowledgements

The authors would like to thank Woodside, Woodside's joint venture participant POSCO DAEWOO, and Myanma Oil and Gas Enterprise (MOGE), for permission to present this work. They also wish to express gratitude towards the FULLWAVE Game Changer JIP at Imperial College London, for their role in developing the FWI engine used. Any views or opinions expressed in this paper are solely those of the authors and do not necessarily represent those of Woodside or S-CUBE.

EDITED REFERENCES

Note: This reference list is a copyedited version of the reference list submitted by the author. Reference lists for the 2017 SEG Technical Program Expanded Abstracts have been copyedited so that references provided with the online metadata for each paper will achieve a high degree of linking to cited sources that appear on the Web.

REFERENCES

Bunks, C., F. M. Saleck, S. Zaleski, and G. Chavent, 1995, Multiscale seismic waveform inversion: Geophysics, **60**, 1457–1473, https://doi.org/10.1190/1.1443880.

Debens, H. A., M. Warner, A. Umpleby, and N. V. da Silva, 2015, Global anisotropic 3D FWI: 85th Annual International Meeting, SEG, Expanded Abstracts, 1193–1197, https://doi.org/10.1190/segam2015-5921944.1.

Harrowfield, G., 2015, Mass transport complexes of the Rakhine Basin, Myanmar – Deepwater examples from recent 3D seismic data: SEAPEX Exploration Conference.

Mancini, F., K. Prindle, T. Ridsdill-Smith, and J. Moss, 2016, Full-waveform inversion as a game changer: Are we there yet? The Leading Edge, **35**, 445–448, 450–451, https://doi.org/10.1190/tle35050445.1.

Tarantola, A., 1984, Inversion of seismic reflection data in the acoustic approximation: Geophysics, **49**, 1259–1266, https://doi.org/10.1190/1.1441754.

Warner, M., and L. Guasch, 2016, Adaptive waveform inversion: Theory: Geophysics, **81**, no. 6, R429–R445, https://doi.org/10.1190/geo2015-0387.1.